ORGANOMETALLICS

ARTICLE

pubs.acs.org/Organometallics

Reductive Coupling of CO Templated by Iron Bound to the Tris(pyrrolide)ethane Scaffold

Graham T. Sazama and Theodore A. Betley*

Department of Chemistry and Chemical Biology, Harvard University, 12 Oxford Street, Cambridge, Massachusetts 02138, United States

Supporting Information

ABSTRACT: The reactivity of the high-spin (S = 2) [(^{Mes}tpe)Fe(THF)][Li(THF)$_4$] (**1**) complex (^{Mes}tpe = tris-(mesitylpyrrolide)ethane) with isocyanide and CO substrates is explored. Reaction of **1** with excess ^{t}BuNC forms a low-spin (S = 0), six-coordinate iron(II) species with three ^{t}BuNC ligands bound to iron, producing a notable tautomerization of one of the pyrrolide units from N- to C-ligation to iron. Reaction of **1** with an atmosphere of CO also produces a new diamagnetic complex, wherein two molecules of CO are consecutively reductively coupled, driven by the two-electron oxidation and fragmentation of the tris(pyrrolide)ethane ligand. The product features a six-coordinate Fe(II) species bound to a dipyrromethene ligand (resulting from oxidative fragmentation of the ^{Mes}tpe ligand), an oxalylimino pyrrole fragment from pyrrole coupling to two molecules of CO. The reactions of **1** with ^{t}BuNC and CO provide insight into how tautomerization of the tris(pyrrolide) ligand upon substrate binding initiates the contiguous reductive coupling of CO.

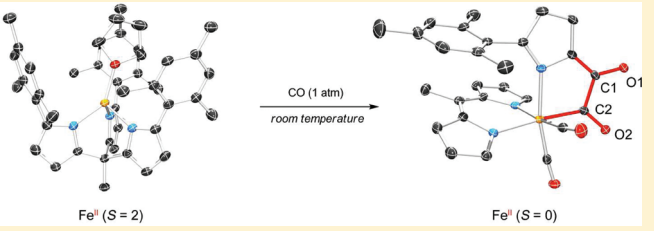

The reduction of CO to form C−C bonds is one of the two key steps involved in the Fischer−Tropsch (FT) process, in which a heterogeneous catalyst combines CO and H_2 to produce long-chain hydrocarbons.[1] Few homogeneous examples of FT-relevant transformations are known, but have provided insight into key challenges associated with FT chemistry: formation of C−C bonds from reduced carbonyl species, C−H bond formation from metal-coordinated CO, and the role of exogenous Lewis acids in promoting CO reduction. The first reports of facile C−C coupling from metal−carbonyl species arose from carbene coupling following hydride or alkyl insertion into early transition metal or lanthanide carbonyls[2,3] or by alkali reduction of metal carbonyl species followed by electrophilic trapping.[4] These reactions require the preparation of highly reducing transition metal hydride species or utilize alkali metal reductants (e.g., Na) to achieve carbonyl reduction. Two recent examples of FT-relevant chemistry employ the formation of strong early transition metal−oxygen bonds as a driving force to cleave the C−O bond and form new C−C bonds.[5] Moving away from strongly reducing early transition metal hydride or alkyl precursors, reductive coupling of metal carbonyls on a Re-based coordination complex was recently reported using a Lewis-acidic, pendant borane to facilitate carbonyl activation via hydride insertion.[6] From these precedents, a desirable reaction sequence would employ coordination complexes that template the construction of C−C bonds from carbonyl ligands without requiring strong chemical reductants. In this vein, we have investigated the reactivity of the electron-rich [(^{Mes}tpe)Fe]$^-$ anion toward carbonyl and isocyanide substrates, leading to a metal-templated reductive coupling of CO initiated by the ligand framework.[7]

Formation of [(^{Mes}tpe)Fe(THF)][Li(THF)$_4$] (**1**) is accomplished by deprotonation of the (^{Mes}tpe)H$_3$ ligand using base (LiN(SiMe$_3$)$_2$, 3.05 equiv) in THF followed by subsequent addition to a thawing slurry of divalent iron chloride in THF (Scheme 1a; THF = tetrahydrofuran). Recrystallization from THF and hexane affords a pale brown-yellow powder in 72% yield. The ^{1}H NMR spectrum reveals **1** to be paramagnetic (solution magnetic moment = 5.56(5) μ_B, consistent with a spin-only value of S = 2),[8] with 10 proton resonances apparent, ranging from δ 80 to −6 ppm. The zero-field ^{57}Fe Mössbauer spectrum (δ = 0.85 mm/s, $|\Delta E_Q|$ = 2.55 mm/s) gives parameters consistent with a high-spin formulation for **1** that are very similar to the previously reported pyridine adduct, [(^{Mes}tpe)Fe(py)]$^-$.[7] X-ray diffraction quality crystals can be obtained from a THF−hexane solution stored for two weeks at −35 °C. The crystal structure (Figure 1) shows the tpe ligand bound κ^3 to the Fe center (Fe−N distances: 2.005(3), 2.028(3), and 2.033(3) Å) with one THF molecule occupying a fourth coordination site (Fe−O bond length = 2.023(2) Å).[9] The Fe-bound THF molecule is parallel to two mesityl fragments and canted away from the third, and thus does not fall on the molecular-C_3 axis (defined by the vector containing the tpe ligand bridgehead and the Fe center), giving an overall pseudotetrahedral geometry at iron. A similar deviation from C_3 symmetry was also observed in the reported pyridine complexes; however in the pyridine complexes this can be attributed to a significant π-stacking interaction with a ligand mesityl unit not present in the THF complex.[7]

Received: May 9, 2011
Published: July 19, 2011

Scheme 1[a]

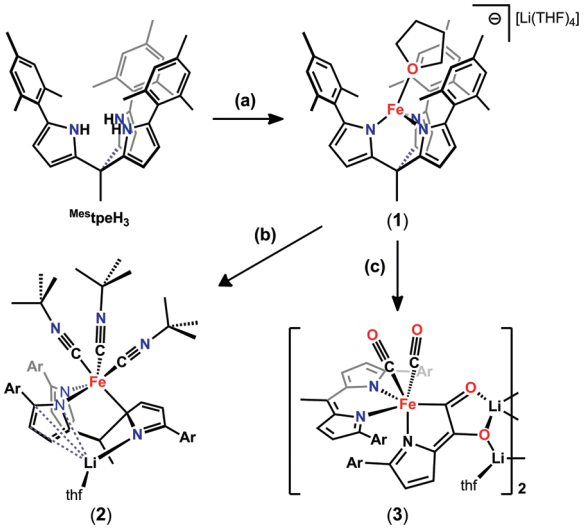

[a] Reaction conditions: (a) 1. $LiN(SiMe_3)_2$ (3.05 equiv), THF, 25 °C, 1.5 h; 2. $FeCl_2$ (1.1 equiv), thawing THF, 3 h; (b) ^tBuNC (3.3 equiv), benzene, 25 °C; (c) CO gas (1 atm), benzene, 25 °C.

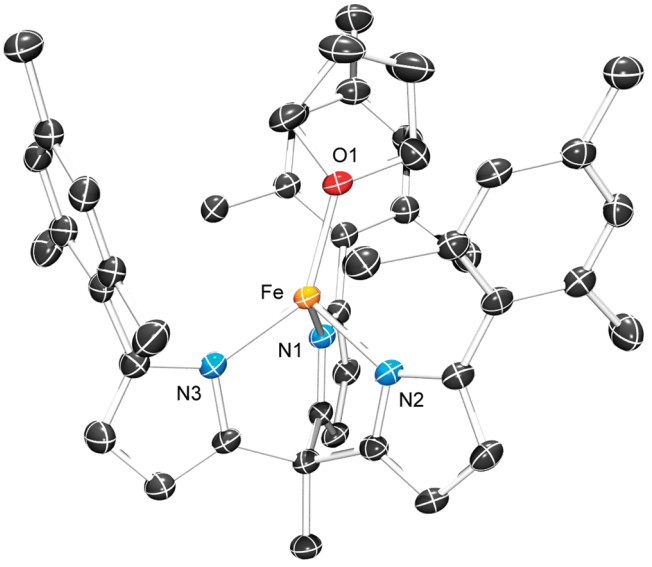

Figure 1. Solid-state molecular structure for $[(^{Mes}tpe)Fe(THF)]^-$ (**1**) (thermal ellipsoids shown at 50% probability and hydrogens and THF-bound lithium counterion omitted for clarity). Selected bond lengths (Å) and angles (deg): Fe—N1 2.033(3); Fe—N2 2.028(3); Fe—N3 2.005(3); Fe—O 2.023(2); N1—Fe—N2 93.93(11); N1—Fe—N3 95.39(11); N2—Fe—N3 95.37(11).

Reaction of **1** with *tert*-butylisocyanide (^tBuNC, 3.3 equiv) at room temperature in benzene immediately resulted in the precipitation of a bright orange powder (92% yield, Scheme 1b). The product, $[(^{Mes}tpe)Fe(CN^tBu)_3]Li(THF)$ (**2**), was sparingly soluble in benzene, but saturated solutions of **2** in C_6D_6 were sufficient for obtaining assignable ^1H NMR spectra. The ^1H NMR spectrum of **2** revealed a diamagnetic species, which was reflected in the marked shift of the spectral parameters obtained for **2** in the ^{57}Fe Mössbauer spectrum (δ = 0.12 mm/s, $|\Delta E_Q|$ = 0.47 mm/s). The significant decrease in isomer shift

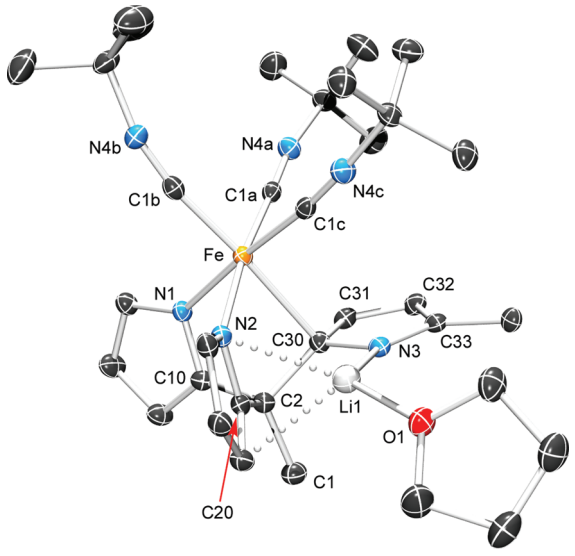

Figure 2. Solid-state molecular structure of $[(N,N,C\text{-}^{Mes}tpe)Fe(CN^tBu)_3]Li(THF)$ (**2**, thermal ellipsoids shown at 50% probability and hydrogens and mesityl groups omitted for clarity). Selected bond lengths (Å) and angles (deg) for **2**: Fe1—N1 2.0180(16); Fe1—N2 2.0538(17); Fe1—C30 2.2531(19); C1a—N4a 1.166(3); C1b—N4b 1.166(3); C1c—N4c 1.162(3); N3—C30 1.421(3); C30—C31 1.433(3); C31—C32 1.376(3); C32—C33 1.430(3); C33—N3 1.333(3); C2—C10 1.499(3); C2—C20 1.504(3); C2—C30 1.548(3); N1—Fe—N2 87.82(7), N1—Fe—C30 79.31(7), N2—Fe—C30 78.62(7). Dihedral angle: C10—C2—C1—C20 122.36°.

results from a spin-state change (from S = 2 for **1** to S = 0 for **2**) and back-bonding from Fe to three π-acidic isonitrile ligands. The large decrease observed in the quadrupole splitting is likewise attributable to the change in spin state, wherein the asymmetric population of the e set in the approximately tetrahedral **1** ($(e)^3(t_2)^3$) changes to the electronically symmetric, octahedral coordination in **2** $(t_{2g})^6(e_g)^0$.

Large, translucent, deep red crystals of X-ray diffraction quality of **2** grew from saturated benzene solutions standing overnight at room temperature under an inert atmosphere. The X-ray diffraction crystal structure of **2** shows three bound isonitrile molecules (see Figure 2). The isonitrile C—N distances are between 1.162(3) and 1.166(3) Å, and a strong, broad FTIR absorbance (ν_{C-N}) was observed at 2093 cm^{-1} (free isonitrile ν_{C-N} = 2137 cm^{-1}), indicative of weak π-back-bonding from the low-spin iron(II). Most striking about the structure of **2** is the observed tautomerization of one pyrrolide unit, resulting in pyrrole *C*-ligation to Fe (Fe1—C30, 2.253(2) Å) and the now imino nitrogen (N3—C33: 1.333(3) Å, consistent with a C=N formulation) bound to lithium (N3—Li: 2.253(2) Å). The lithium cation is bound η^5 to a neighboring pyrrolide unit (C/N—Li distances range from 2.250(4) to 2.578(4) Å) and one molecule of THF. The pyrrole *C*-ligation to iron produces a bond contraction of 0.035 Å of two backbone—pyrrole bonds (C2—C10 and C2—C20, from 1.536(5) and 1.537(5) Å in **1** to 1.499(3) and 1.504(3) Å in **2**). This change suggests a strengthening of the pyrrole—backbone connection with two pyrroles, providing evidence that this mode of ligation is intermediate between the *N,N,N*-ligation and a dipyrromethene. The change in (^{Mes}tpe) ligand hapticity from *N,N,N*-ligation to *N,N,C*-ligation likely arises from the inability of the (^{Mes}tpe) to accommodate the three large isocyanide ligands. While the steric

dx.doi.org/10.1021/om2003859 |*Organometallics* 2011, 30, 4315–4319

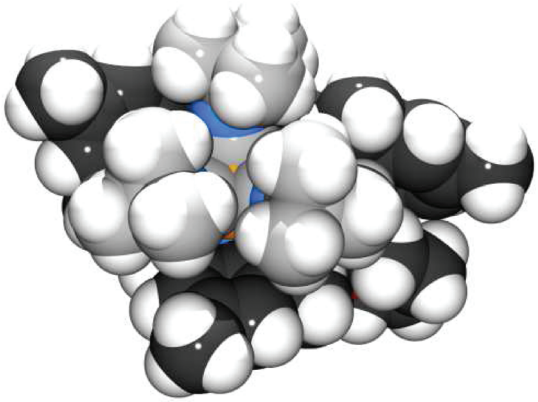

Figure 3. Space-filling model of **2** where the three ^{t}BuNC carbon atoms are colored gray and the (^{Mes}tpe) ligand carbon atoms are colored black.

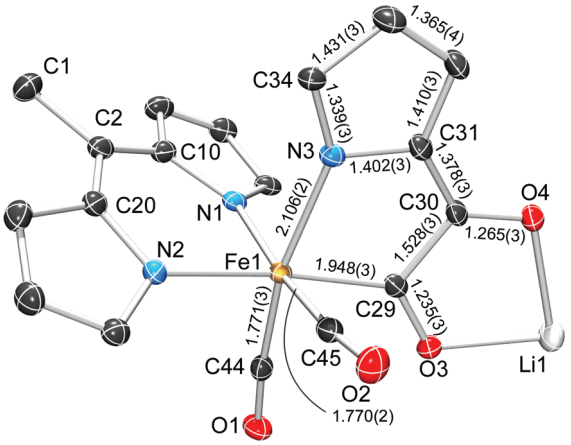

Figure 4. Solid-state molecular structure of one-half of the dimeric structure for {[(^{Mes}dpme)Fe(CO)$_2$(^{Mes}NC$_4$H$_2$-C(O)C(O))]Li}$_2$ (**3**) (thermal ellipsoids shown at 50% probability; hydrogens, mesityl groups, one bridging lithium, and solvent molecules omitted for clarity).[12] Selected bond lengths (Å) for **3**: Fe1−N1 2.0267(17); Fe1−N2 2.0823(17). N1−Fe1−N2 bond angle: 88.31(7)°. Dihedral angle C10−C2−C1−C20: 173.36°.

pressure caused by binding of the three *tert*-butylisocyanide ligands is apparent from viewing the space-filling model of **2** (see Figure 3), another, more subtle driving-force is reorganization of the (^{Mes}tpe) trianion to enable octahedral coordination of the bound metal ion. The three N−Fe−N bond angles in high-spin **1** range from 93.93(11)° to 95.39(11)°, but expand to an average of 96.05(7)° in the diamagnetic [(^{Mes}tpe)Zn(py)]$^-$ anion. Upon tautomerizing in **2** to the *N*,*N*,*C*-ligation, the (^{Mes}tpe) bond angles decrease (N1−Fe−N2 87.82(7)°, N1−Fe−C30 79.31(7)°, N2−Fe−C30 78.62(7)°). This change in binding mode provides a greater volume to accommodate the three linear *tert*-butylisocyanide ligands, facilitating the octahedral coordination at iron in **2**.

Exposure of **1** to one atmosphere of CO gas affords a markedly different product from **2** that is soluble in most organic solvents (Scheme 1c). ^{1}H and ^{13}C NMR (C_6D_6 solution) and Mössbauer spectra of this product represent a clean diamagnetic material, with desymmetrization of the ligand environment apparent by ^{1}H NMR. FTIR spectroscopy reveals four absorption bands at 1960, 1816, 1528, and 1480 cm^{-1}, where the first two are likely assignable to the C−O stretches of terminally bound carbonyl ligands (free CO ν_{CO} = 2143 cm^{-1}). The latter two stretching frequencies are consistent with ketone-like functionalities. The Mössbauer parameters obtained for **3** (δ = 0.06 mm/s and $|\Delta E_Q|$ = 1.20 mm/s) are similar to those obtained for **2**. The low isomer shift (relative to that obtained for **1**, 0.85 mm/s) reflects a likely spin-state change analogous to that observed in **2**, with the addition of π-back-bonding to CO ligands. Changes in the quadrupole splitting, while less pronounced than in **2**, again reflect a change from high-spin to low-spin Fe^{2+}.

Crystals suitable for X-ray crystallography can be grown from a C_6D_6 solution after standing for two weeks at room temperature under one atmosphere of CO. The crystal structure reveals that the product, {[(^{Mes}dpme)Fe(CO)$_2$(^{Mes}NC$_4$H$_2$-C(O)C(O))]Li}$_2$ (**3**, Figure 4, full structure available in SI), is a dimer of mononuclear iron complexes in which the tpe ligand has undergone oxidative fragmentation to form a dipyrromethene fragment[10] and a separate, dicarbonylated pyrrole unit. The pyrrole unit has nucleophilically coupled two reactant CO molecules, forming a bidentate, oxalyl-imino moiety, giving rise to the two lower carbonyl stretching frequencies observed in the IR spectrum of **3**. The two mononuclear Fe complexes are bridged via lithium cations bound to the two oxalato-oxygens (O3 and O4 in Figure 1c), with a crystallographic C_2 symmetry axis through the lithium atoms. Two molecules of THF complete the coordination sphere for the lithium bridging via only one oxalato oxygen (see full structure, available in SI). Bond lengths suggest an imino formulation of the pyrrole nitrogen (N3−C34 = 1.339(3) Å, consistent with a C−N double bond). This fragment contains π-bonds conjugated through the pyrrole-oxalyl fragment (see Scheme 1, **3**), terminating in an acyl carbon bound to iron (Fe1−C29 = 1.948(3) Å). The two unfunctionalized bound CO molecules display C−O bond lengths of 1.144(3) and 1.150(3) Å, similar to lengths seen for other low-spin Fe^{2+} dicarbonyl complexes reported in the literature.[11]

The information obtained from the crystal structure data for complexes **2** and **3** allow us to propose a reaction mechanism for the formation of **3** from **1** (Scheme 2). We propose that upon coordination of 3 equiv of CO, **1** initially forms a tautomer intermediate analogous to the structure of **2** (Scheme 2, **2a**). The nucleophilic carbon-bound pyrrole subunit migrates to a bound carbonyl to form a four-membered aza-metallacyclobutene (**2b**), oxidizing the (^{Mes}tpe) trianion to the monoanionic dipyrromethene.[13] The enolate-like structure of proposed intermediate **2b** migrates to a second bound carbonyl, forming an α,*β*-diketo-azametallacyclopentane (**2c**), presumably to relieve steric strain from the aza-metallacyclobutene intermediate **2b**, which subsequently undergoes tautomerization to form the thermodynamically stable imino-acyl dimer product **3**. The steric bulk of the *tert*-butylisocyanide ligands in **2** likely prevents the formation of C−C coupled product akin to **3**,[14] arresting the above reaction sequence at the ligand tautomer **2**.

The proposed mechanism necessitates a closer inspection of the role of lithium in the reductive coupling process. Given the precedent for Lewis-acid activation of CO,[6,15,16] the lithium cation could bind and activate a bound CO toward nucleophilic attack. In opposition to this, however, the CO coupling reaction proceeds even in THF solutions, which should sequester the Li$^+$ and preclude Lewis-acid activation of a CO ligand. Alternatively, the presence of Li$^+$ may facilitate the formation of tautomer **2a**, priming the nucleophile for the observed reductive coupling. Substitution of the lithium for bulky, noncoordinating cations

dx.doi.org/10.1021/om2003859 |*Organometallics* 2011, 30, 4315–4319

Scheme 2. Proposed Mechanism of CO Reductive Coupling Reaction

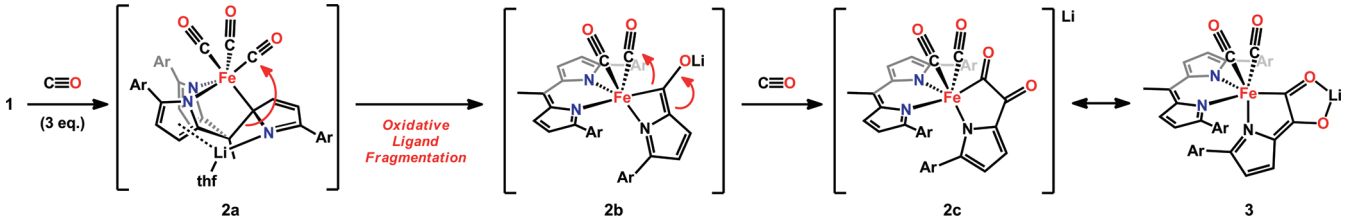

(e.g., PPh_4^+, $[Ph_3P{=}N{=}PPh_3]^+$) results in highly insoluble species, but further examination may yet still elucidate the role of lithium in the coupling process.

We have observed the reductive coupling of two CO ligands under mild reaction conditions (1 atm of CO), without the use of strong exogenous reducing agents.[16] The hapticity change of the (^{Mes}tpe) trianion facilitates coordination environment changes at the metal ion, where *N,N,N*-ligation is preferred for tetrahedral complexes and *N,N,C*-ligation preferentially stabilizes an octahedral field. The facile interchange of the ligand coordination mode generates a metal-bound nucleophile to trigger migration to a metal-bound carbonyl, giving rise to CO reduction with concomitant (^{Mes}tpe) oxidative fragmentation in the absence of an alkali metal reductant. A second carbonyl coupling is likely facilitated by the strained four-membered azametallacycle formed via the initial carbonyl insertion, where incorporation of a second equivalent of CO results in a more stabilized five-membered oxalyl-imino pyrrole product. The results presented herein allude to more general reactions based on a ligand platform similar to that found in the final product and employing extant nucleophiles; this possibility is especially appealing given our group's concurrent research into the chemistry of dipyrromethene complexes. We are currently pursuing further investigation of generalization of this reactivity.

EXPERIMENTAL SECTION

All manipulations were carried out in the absence of water and dioxygen using standard Schlenk techniques or in an MBraun inert atmosphere glove box under a dinitrogen atmosphere. All glassware was oven-dried for a minimum of 1 h and cooled in an evacuated antechamber prior to use in the glove box. Benzene, diethyl ether, *n*-hexane, tetrahydrofuran, and toluene were dried and deoxygenated on a Glass Contour System (SG Water USA, Nashua, NH) and stored over 4 Å molecular sieves (Strem) prior to use. Benzene-d_6 was purchased from Cambridge Isotope Laboratories and degassed and stored over 4 Å molecular sieves prior to use. Pyridinium *p*-toluenesulfonate, ferrocenium hexafluorophosphate, dihydroanthracene, and anhydrous pyridine were purchased from Aldrich and used as received. Anhydrous iron(II) chloride was purchased from Strem and used as received. Celite 545 (J. T. Baker) and 4 Å molecular sieves were dried in either a Schlenk flask or a vacuum oven for 24 h under dynamic vacuum while heating to at least 150 °C.

Characterization and Physical Measurements. ^{1}H and ^{13}C NMR spectra were recorded on Varian Mercury 400 MHz or Varian Unity/Inova 500 MHz spectrometers. ^{1}H and ^{13}C NMR chemical shifts are reported relative to residual solvent peaks as reference. Elemental Analyses were carried out at Complete Analysis Laboratories, Inc. (Parsippany, NJ).

^{57}Fe Mössbauer spectra were measured with a constant acceleration spectrometer (SEE Co, Minneapolis, MN). Isomer shifts are quoted relative to Fe metal at room temperature. Data were analyzed and simulated with Igor Pro 6 software (WaveMetrics, Portland, OR) using Lorentzian fitting functions.

X-ray Crystallography Procedures. All structures were collected on a Bruker three-circle platform goniometer equipped with either a Bruker Apex I or Apex II CCD and an Oxford Cryostream cooling device. Radiation was from a graphite fine-focus sealed tube Mo Kα (0.71073 Å) source. Crystals were mounted on a cryoloop using Paratone-*N* oil. All structures were collected at 100 K. Data were collected as a series of φ and/or ω scans. Data were integrated using SAINT (Bruker AXS) and scaled with a multiscan absorption correction using SADABS (Bruker AXS).[17] The structures were solved by direct methods or Patterson maps using SHELXS-97[18] and refined against F^2 on all data by full matrix least-squares with SHELXL-97. All nonhydrogen atoms were refined anisotropically. Hydrogen atoms were placed at idealized positions and refined using a riding model. The isotropic displacement parameters of all hydrogen atoms were fixed to 1.2 times the *U* value of the atoms they are linked to (1.5 times for methyl groups). Further details on several structures are noted below. **Note on 2:** The structure of **2** contained a Li-bound THF that exhibited positional disorder. No restraints were necessary to refine the model. The major component of the disordered THF refined to 75%. **Note on 3:** A free benzene solvent molecule was disordered over two positions and refined with the aid of similarity restraints, with the major contributor refining to 68%. **Note on 4:** The structure of **4** contained a Li-bound THF that exhibited positional disorder. EADP, SIMU, and DELU restraints were used to refine the model, and the two parts refined to 50% each.

[(tpe)Fe(THF)][Li(THF)$_4$] (***1***). In separate 20 mL scintillation vials, tris(pyrrolyl)ethane (^{Mes}tpeH$_3$, 0.635 g, 1.10 mmol) and Li(N(SiMe$_3$)$_2$) (0.554 g, 3.31 mmol) were each dissolved in 4 mL of THF. The solution of Li(N(SiMe$_3$)$_2$) was added to the solution of tpeH$_3$ and stirred at room temperature for 1 h. In another 20 mL vial $FeCl_2$ (0.166 g, 1.31 mmol) was slurried in 2 mL of THF. Both vials were placed in a liquid nitrogen cooled cold well until frozen. The ligand solution was thawed and added to the stirring slurry of $FeCl_2$. The reaction mixture became a translucent dark brown solution as it warmed. The reaction was stirred at room temperature for 2 h, after which removal of the solvent *in vacuo* gave a brown residue. The residue was extracted into 5 mL of diethyl ether and filtered through diatomaceous earth to remove lithium chloride. THF (5 drops) was added to the dark brown ether filtrate, and a yellow-brown precipitate (**1**) formed. The solution was cooled to −35 °C overnight, and the precipitate was collected on a medium fritted funnel. The solid was purified by precipitation from THF with hexane, and 0.729 g (72% yield) of yellow powder was collected and stored at −35 °C. Crystals suitable for X-ray diffraction were grown from a mixture of THF and hexane at −35 °C. ^{1}H NMR (400 MHz, C_6D_6): δ/ppm: 78.84 (br s), 69.79 (br s), 48.22 (br s), 28.81 (br s), 26.69 (sh), 12.91 (br s), 4.10 (br s), 1.61 (br s), 1.02 (br s), −5.39 ppm (br s). Comb. Anal. Calcd for $[C_{45}H_{50}FeN_3O]^-[LiC_{16}H_{32}O_4]^+$: C, 73.25; H, 8.26; N, 4.20. Found: C, 73.19; H, 8.08; N, 4.31.

[(tpe)Fe(CN^{t}Bu)$_3$]Li(THF) (***2***). A benzene solution of *tert*-butyl isocyanide (28.3 mg, 0.340 mmol) was added to a benzene solution of **1** (103.7 mg, 0.1037 mmol) and stirred two hours at room temperature.

dx.doi.org/10.1021/om2003859 |*Organometallics* 2011, 30, 4315–4319

A bright orange precipitate formed out of the dark red-orange solution and was collected and dried on a medium fritted funnel (91.4 mg, 92%). Crystals suitable for X-ray diffraction were grown from a solution of **2** in C_6D_6 at room temperature in an NMR tube. ^{1}H NMR (500 MHz, C_6D_6): δ/ppm 7.88 (d), 6.99 (s), 6.93 (s), 6.80 (m), 6.50 (s), 6.37 (s), 6.04 (s), 2.70 (s), 2.34 (m), 2.25 (s), 2.19 (s), 1.80 (s) 1.13 (s), 0.95 (s), 0.89 (s). Comb. Anal. Calcd for $C_{60}H_{77}FeLiN_6O$: C, 74.98; H, 8.08; N, 8.74. Found: C, 74.86; H, 8.01; N, 8.59.

[(dpme)Fe(COCOC$_4$H$_2$NMes)]$_2$[Li(THF)]$_2$ (**3**). A 100 mL recovery flask was charged with a 10 mL benzene solution of **1** (357.3 mg, 357.3 mmol) and sealed with a fresh rubber septum under nitrogen. Carbon monoxide gas (35 mL at 1 atm, 1.43 mmol) was added via syringe to the flask, and the reaction mixture was stirred for one hour at room temperature. The solution was frozen and lyophilized, and 343.2 mg of dark red-brown powder was isolated. The resultant powder was purified by dissolving in hexane, filtering through diatomaceous earth to remove unreacted **1**, and collecting and evaporating the filtrate *in vacuo*, providing dark red-brown **3** as a powder. X-ray diffraction quality crystals were grown in saturated C_6D_6 solutions over a period of 2 weeks. ^{1}H NMR (500 MHz, C_6D_6): δ/ppm 7.38 (d, J = 4.4 Hz, 1 H), 7.24 (br s, 1 H), 7.03 (d, J = 4.4 Hz, 2 H), 6.90 (br s, 2 H), 6.75 (s, 1 H), 6.77 (s, 1 H), 6.51 (br s, 1 H), 6.39 (d, J = 3.9 Hz, 1 H), 6.27 (d, J = 3.9 Hz, 1 H), 6.22 (d, J = 4.4 Hz, 1 H), 3.53 (br s, 9 H), 2.71 (s, 3 H), 2.40 (s, 3 H), 2.25−2.34 (m, 6 H), 2.13−2.24 (m, 9 H), 1.97 (s, 6 H), 1.80 (s, 3 H), 1.36 (br s, 9 H). ^{13}C NMR (126 MHz, C_6D_6): δ/ppm 212.4, 211.8, 184.8, 171.3, 164.9, 163.2, 161.9, 149.2, 142.8, 142.1, 140.8, 139.2, 138.9, 138.2, 138.0, 137.5, 137.2, 136.8, 136.7, 136.4, 135.2, 130.1, 129.8, 129.3, 129.0, 128.9, 128.1, 127.9, 127.4, 124.8, 123.0, 120.3, 119.6, 68.5, 26.0, 22.9, 22.8, 22.2, 22.2, 22.1, 21.8, 21.7, 21.6, 21.5, 20.7, 3.0. Comb. Anal. Calcd for $C_{49}H_{50}FeLiN_3O_5$: C, 71.45; H, 6.12; N, 5.10. Found: C, 71.33; H, 6.13; N, 5.19.

■ ASSOCIATED CONTENT

Supporting Information. X-ray crystallographic data for **1**−**3**. This material is available free of charge via the Internet at http://pubs.acs.org.

■ AUTHOR INFORMATION

Corresponding Author
*E-mail: betley@chemistry.harvard.edu.

■ ACKNOWLEDGMENT

The authors thank Harvard University and the NSF (CHE-0955885) for financial support (T.A.B.), the NSF for a predoctoral fellowship (G.T.S.), and Dr. Shao-Liang Zheng for his assistance with X-ray crystallography.

■ REFERENCES

(1) Khodakov, Y.; Chu, W.; Fongarland, P. *Chem. Rev.* **2007**, *107*, 1692.

(2) (a) Manriquez, J. M.; McAlister, D. R.; Sanner, R. D.; Bercaw, J. E. *J. Am. Chem. Soc.* **1976**, *98*, 6733. (b) Calderazzo, F. *Angew. Chem., Int. Ed. Engl.* **1977**, *16*, 299. (c) Fachinetti, G.; Floriani, C.; Roselli, A.; Pucci, S. *J. Chem. Soc., Chem. Commun.* **1978**, 269. (d) Labinger, J. A.; Wong, K. S.; Scheidt, R. *J. Am. Chem. Soc.* **1978**, *100*, 3254. (e) Wood, C. D.; Schrock, R. R. *J. Am. Chem. Soc.* **1979**, *101*, 5421. (f) Wolczanski, P. T.; Bercaw, J. E. *Acc. Chem. Res.* **1980**, *13*, 121. (g) Barger, P. T.; Santarsiero, B. D.; Armantrout, R.; Bercaw, J. E. *J. Am. Chem. Soc.* **1984**, *106*, 5178. (h) Erker, G. *Acc. Chem. Res.* **1984**, *17*, 103. (i) Toreki, R.; LaPointe, R. E.; Wolczanski, P. T. *J. Am. Chem. Soc.* **1987**, *109*, 7558. (j) Hofmann, P.; Stauffert, P.; Frede, M.; Tatsumi, K. *Chem. Ber.* **1989**, *122*, 1559. (k) Miller, R. L.; Toreki, R.; LaPointe, R. E.; Wolczanski, P. T.; Van Duyne, G. D.; Roe, D. C. *J. Am. Chem. Soc.* **1993**, *115*, 5570. (l) Wolczanski, P. T. *Polyhedron* **1995**, *14*, 3335.

(3) (a) Manriquez, J. M.; Fagan, P. J.; Marks, T. J.; Day, C. S.; Day, V. W. *J. Am. Chem. Soc.* **1978**, *100*, 7112. (b) Marks, T. J. *Prog. Inorg. Chem.* **1979**, *25*, 224. (c) Fagan, P. J.; Manriquez, J. M.; Marks, T. J. In *Organometallics of the f-Elements*; Marks, T. J.; Fischer, R. D., Eds.; Reidel Publishing Co.: Dordrecht, Holland, 1979; Chapter 4. (d) Fagan, P. J.; Manriquez, J. M.; Marks, T. J.; Day, V. W.; Vollmer, S. H.; Day, C. S. *J. Am. Chem. Soc.* **1980**, *102*, 5393. (e) Katahira, D. A.; Moloy, K. G.; Marks, T. J. *Organometallics* **1982**, *1*, 1723.

(4) (a) Lam, C. T.; Corfield, P. W. R.; Lippard, S. J. *J. Am. Chem. Soc.* **1976**, *21*, 91. (b) Bianconi, P. A.; Williams, I. D.; Engeler, M. P.; Lippard, S. J. *J. Am. Chem. Soc.* **1986**, *108*, 311. (c) Bianconi, P. A.; Vrtis, R. N.; Rao, Ch. P.; Williams, I. D.; Engeler, M. P.; Lippard, S. J. *Organometallics* **1987**, *6*, 1968. (d) Carnahan, E. M.; Protasiewicz, J. D.; Lippard, S. J. *Acc. Chem. Res.* **1993**, *26*, 90.

(5) (a) Matsuo, T.; Kawaguchi, H. *J. Am. Chem. Soc.* **2005**, *127*, 17198. (b) Shima, T.; Hou, Z. *J. Am. Chem. Soc.* **2006**, *128*, 8124.

(6) (a) Miller, A. J. M.; Labinger, J. A.; Bercaw, J. E. *J. Am. Chem. Soc.* **2008**, *130*, 11874. (b) Miller, A. J. M.; Labinger, J. A.; Bercaw, J. E. *J. Am. Chem. Soc.* **2010**, *132*, 3301. (c) Miller, A. J. M.; Labinger, J. A.; Bercaw, J. E. *Organometallics* **2010**, *29*, 4499.

(7) Sazama, G. T.; Betley, T. A. *Inorg. Chem.* **2010**, *49*, 2512.

(8) Evans, D. F. *J. Chem. Soc.* **1959**, 2003.

(9) Compound **1**: $C_{61}H_{82}FeLiN_3O_5$, M_r = 1000.09, monoclinic, $P2(1)/c$, a = 13.875(5) Å, b = 24.856(9) Å, c = 15.973(6) Å, α = 90°, β = 94.945(8)°, γ = 90°, V = 5488(3) Å^3, Z = 4, ρ_{calcd} = 1.210 Mg/m^3, μ = 0.326 mm^{-1}, $R_1(I > 2\sigma(I))$ = 0.0630, wR_2 = 0.1508, GOF = 1.107. Compound **2**: $C_{69}H_{86}FeLiN_6O$, M_r = 1078.23, triclinic, $P\bar{1}$, a = 10.7409(7) Å, b = 12.5697(8) Å, c = 23.8076(15) Å, α = 88.352(4)°, β = 84.975(4)°, γ = 72.407(4)°, V = 3052.1(3) Å^3, Z = 2, ρ_{calcd} = 1.173 Mg/m^3, μ = 0.294 mm^{-1}, R_1 ($I > 2\sigma(I)$) = 0.0536, wR_2 = 0.1113, GOF = 1.016. Compound **3**: $C_{47}H_{57}Fe_3N_6P_3$, M_r = 966.45, monoclinic, $C2/c$, a = 25.163(4) Å, b = 10.6991(16) Å, c = 34.829(5) Å, α = 90°, β = 90.582(3)°, γ = 90°, V = 9376(2) Å^3, Z = 8, ρ_{calcd} = 1.278 Mg/m^3, μ = 0.374 mm^{-1}, $R_1(I > 2\sigma(I))$ = 0.0566, wR_2 = 0.1159, GOF = 1.035. CCDC-788652 (**1**), 788653 (**2**), 788654 (**3**) contain the supplementary crystallographic data for this paper. These data can be obtained free of charge from the Cambridge Crystallographic Data Centre via www.ccdc.cam.ac.uk/data_request/cif.

(10) King, E. R.; Betley, T. A. *Inorg. Chem.* **2009**, *48*, 2361.

(11) (a) Bart, S. C.; Chłopek, K.; Bill, E.; Bouwkamp, M. W.; Lobkovsky, E.; Neese, F.; Wieghardt, K.; Chirik, P. J. *J. Am. Chem. Soc.* **2006**, *128*, 13901. (b) Vendemiati, B.; Prini, G.; Meetsma, A.; Hessen, B.; Teuben, J. H.; Traverso, O. *Eur. J. Inorg. Chem.* **2001**, *2001*, 707.

(12) Additional structural details are available in SI.

(13) Although we cannot rule out the formation of a metallocyclopropane followed by tautomerization, this transformation seems unlikely to occur due to the steric constraints of the ^{Mes}tpe ligand.

(14) Berg, F. J.; Petersen, J. L. *Organometallics* **1991**, *10*, 1599.

(15) (a) Butts, S. B.; Holt, E. M.; Strauss, S. H.; Alcock, N. W.; Stimson, R. E.; Shriver, D. F. *J. Am. Chem. Soc.* **1979**, *101*, 5864. (b) Collman, J. P.; Finke, R. G.; Cawse, J. N.; Brauman, J. I. *J. Am. Chem. Soc.* **1978**, *100*, 4766.

(16) (a) Wong, A.; Atwood, J. D. *J. Organomet. Chem.* **1980**, *199*, C9. (b) Wong, A.; Atwood, J. D. *J. Organomet. Chem.* **1981**, *210*, 395. (c) Okazaki, M.; Ohtani, T.; Inomata, S.; Tagaki, N.; Ogino, H. *J. Am. Chem. Soc.* **1998**, *120*, 9135.

(17) Bruker AXS. *APEX II*; Bruker AXS: Madison, WI, 2009.

(18) Sheldrick, G. M. *Acta Crystallogr.* **2008**, *A64*, 112–122.